



A System for Real-Time Syringe Classification and Volume Measurement Using a Combination of Image Processing and Artificial Neural Networks

Hem K. Regmi¹ · Jerry Nesamony² · Scott M. Pappada^{3,4} · Thomas J. Papadimos³ · Vijay Devabhaktuni¹

Published online: 22 October 2018

© Springer Science+Business Media, LLC, part of Springer Nature 2018

Abstract

Purpose The purpose of this research was to develop a system that can read and report the volume of liquid medication present in syringes.

Methods The system is comprised of a digital webcam which is designed to communicate with a computer program developed using MATLAB. The system includes two functional modules, one supporting syringe classification, and another supporting volume measurement. Adaptive template matching was used to determine the best match point between target and template images. The connected component labeling method was used during volume measurement. An artificial neural network (ANN) model was developed using MATLAB to support the intended volume measurement functionality. The developed ANN was designed as a classifier which determines the plunger depth of the syringe and then leverages this result to calculate and derive the volume of medication inside the syringe as the final system output. Commercial Luer-lock syringes of sizes from 1 to 30 ml were used in conjunction with syringe tip caps of blue and yellow color. Tap water or aqueous dye solutions of yellow, red, and blue color simulated liquid medication in the syringe.

Results The developed syringe classification system successfully detected and categorized all tested syringes according to their size. The best accuracy of the system was found to be 99.95% with a 3-ml syringe, while the worst accuracy was 95.82% with a 5-ml syringe. It took approximately 6 s to perform the entire task demonstrating the utility of this system to report volumes in real time.

Conclusion The developed system can be used across a variety of settings that routinely support measuring and handling liquids in syringes including hospitals, pharmacies, and the pharmaceutical industry.

Keywords Compounded sterile preparations · Real-time measurement · Syringe volume · Dose accuracy · Image analysis · Artificial neural networks

Hem Regmi and Jerry Nesamony have equal contribution.

Electronic supplementary material The online version of this article (<https://doi.org/10.1007/s12247-018-9358-5>) contains supplementary material, which is available to authorized users.

✉ Jerry Nesamony
jerry.nesamony@utoledo.edu

¹ Electrical Engineering and Computer Science Department, College of Engineering, MS 308, University of Toledo, 2801 W. Bancroft Street, Toledo, OH 43606-3390, USA

² Department of Pharmacy Practice, MS 1013, College of Pharmacy and Pharmaceutical Sciences, University of Toledo HSC, 3000 Arlington Avenue, Toledo, OH 43614, USA

³ Department of Anesthesiology, College of Medicine and Life Sciences, University of Toledo HSC, 3000 Arlington Avenue, Toledo, OH 43614, USA

⁴ Department of Bioengineering, College of Engineering, MS303, University of Toledo, 2801 W. Bancroft Street, Toledo, OH 43606-3390, USA

Introduction

In hospitals and other institutional settings, injections, and parenteral drug delivery is an important means of administering medications to patients. Recently, there has been an increase in the number of medications that are prepackaged in syringes that are sealed with a syringe tip cap. In all these instances, a liquid solution of the drug or diluent is taken in a syringe during compounding, while adding a diluent, when administering the medication to a patient, or when packaging injections or solutions after preparation. The accuracy of the volume of liquid present in the syringe can have a significant effect on the outcome related to the process in which the syringe is intended to be used [1]. For example, if a 500-mg dose is to be provided in 5 ml solution and the actual volume drawn into the syringe was 4.8 ml, there will be a 4% error in the intended dosage to be administered. Such inaccuracies in dose can

impact the therapeutic effect related to a drug [2]. Errors related to inaccurate volume do not occur deliberately; rather a technician or pharmacist can make a genuine mistake. The manual and visual verification of the volume of liquid in a syringe is very subjective resulting in errors due to differences in syringe holding technique and visual inspection of syringe plunger position above or below eye level to name a few [3]. Additionally, numerous pharmaceutical products, including pain medications, hormones, diluents, biotechnology-derived products, anticoagulants, etc., are available in prepackaged syringes or “prefilled syringes.” The imprecision related to the fill volume in prefilled syringes can significantly alter the dosage of the medication based on deviations from the label claim associated with the product [4].

Compounded pharmaceutical preparations are in general reported to be highly error prone with potency being the most common quality testing failure observed, which has been found to range between 68 and 268% of the labeled claim [5]. Compounding of sterile preparations is associated with severe risk factors due to the high incidence and potential for process-based errors [6, 7]. One such heightened degree of risk is because numerous IV medications, such as epinephrine, phenylephrine, norepinephrine, heparin, ketamine, IV anticoagulants, insulin, cardioplegic solutions, hypertonic dextrose, etc., are in the Institute for Safe Medication Practices (ISMP) list of high-risk medications [8]. The high-risk medication list includes all medications that can cause significant patient harm when used in error. Another cause for concern is that erroneous IV medications are directly introduced into the systemic circulation thus triggering potential adverse effects immediately with limited or no possibility of rapid reversal or mitigation [6]. Although not directly attributable to errors made in an IV compounding room, another cause that amplifies the situation are the challenges involved in implementing and using standardized doses of medications [6]. Even when hospital formularies have established definite standardized doses for medications, prescribers have been found to order non-standard doses that require compounding [9]. This practice is thought to be a leading cause of medication errors in therapies administered to adults, children, and neonates. Numerous technology-based solutions have been adopted by other fields in the healthcare industry to address some of the shortcomings in the delivery of patient care. However, a recent survey reported that use of innovative technologies in an IV compounding setting is severely limited across the nation [10]. There are also numerous variants of a particular process that are used in the IV compounding settings across hospitals nationally, contributing to higher occurrence of errors [11]. Lack of regulatory authority related to guidelines published by various stakeholders in this field and the

generalizations used in USP <797> that lend themselves to different interpretations contribute to this type of variable practice [12].

Current practices in pharmaceutical industry include visual inspection using several strategically positioned digital cameras, X-rays, and various imaging devices to inspect for defects, foreign material, cracks, missing or misapplied stoppers and seals, etc. [13]. Machines can provide visual inspection as effectively as human technicians with the advantage of high speed and throughput. However, human inspection is taken as the standard for visual inspection according to USP <790> [14, 15]. Currently there are no available systems that can automate the volume measurement step required during compounding or packaging of sterile preparations that are to be drawn into a syringe. In this manuscript our team introduces and validates a new semi-automatic system that can be readily integrated with existing technologies. The proposed system includes several key design features such as low cost, high accuracy, high efficiency, and robustness. The scope of automatic volume detection is not limited to health care industry, but similar techniques are already being investigated in industrial sectors, such as visual inspection in soft drink bottling plants [16], printed circuit boards (PCBs) [17], and remote visual inspections of aircraft surfaces [18].

The vision for the system is to automate real-time syringe volume reading during compounding and inspection (completed by a pharmacist) through a combination of digital image processing algorithms and artificial neural networks (ANNs). The proposed approach demonstrates the use of digital camera technology to classify and detect the volume of liquid medication taken in Luer-lock syringes. Syringes normally used during compounding of sterile preparations ranges from 1 to 60 ml. The system reported in this manuscript tested syringes of size from 1 to 30 ml. The experiments were conducted for similar syringes at different times under identical experimental conditions to check the reproducibility of the system and accuracy of volume detection. The system was designed to make it realizable in real time to inspect and measure volume of compounding syringe while the technician is compounding the medication. It can also be utilized to obtain the volume and type information of finished products, such as prefilled syringes in manufacturing settings, or to determine the fill volume in syringes by pharmacists checking the volume after compounding is completed.

Materials and Methods

The system developed during this effort consists of two separate components: an initial syringe classification component followed by the volume measurement component. Syringe classification was done using image analysis and digital image

processing. Subsequently, a trained ANN detects the volume of fluids present in the syringe. The measurement stage is dependent upon the results of the syringe classification stage. Specific information regarding the implementation of the syringe classification and volume measurement stages is included below. Furthermore, we discuss the system validation and testing procedures that were implemented during this initial effort.

Our system processes image frames acquired from a digital camera that is integrated with MATLAB software [19]. The MATLAB program includes image processing and machine learning functionality to classify the type of syringe being used and provide an approximation of the volume of medication present in the syringe. Our digital image processing approach to facilitate detection of the syringe tip cap implements adaptive template matching [20]. The use of adaptive template matching forms the basic foundation to extract features of a syringe from the whole image. Adaptive template matching technique is widely utilized in object detection [21], image registration [22], object tracking [23], as well as within various types of machine vision, industrial, and surveillance applications [24]. In addition to adaptive template matching, we employed a weighted threshold histogram equalization with improved switched median filtering technique [25] to remove the impulse noise in the image and preserved the edge information. A recursive segmentation approach that extends Otsu's method [26] was used to extract the brightest object from the darkest background at the final iteration [27]. Subsequently, a segmentation process converted the gray-scaled image into binary data enabling further processing. Lastly, connected component labeling (CCL) [28] was applied to separate the medication and/or plunger region of the syringe from the whole segmented binary image. Various popular algorithms for CCL were used, tested, and verified in real-time using various hardware interfaces [29]. The multi-class confidence level in conjunction with weighted minimum distance classifier [30] was used to classify six syringes used in the compounding process with considerable accuracy. The feature vectors for all the syringes were widely spaced, enhancing the efficiency and computation time related to the classifier [31].

The automated volume measurement capability of the system is accomplished by using supervised machine learning and ANNs [32]. ANNs were trained to measure the plunger depth in pixels and corresponding volume to build a neural network model that was later utilized for volume calculation. All ANNs were trained using previously established datasets obtained by conducting various experiments to record the plunger length of different syringes at different volumes under identical experimental environments. Support vector machines (SVMs) [33] can perform better than ANNs for training in machine learning due to their higher feature dimensions [34] in analysis. But SVMs are slow and very complex to implement. Additionally, for single input-single output

datasets with high linearity, ANNs can be satisfactorily trained and used.

Commercial Luer-lock syringes of various capacities from 1 to 30 ml were tested using the system. The flow chart illustrating the system and its functioning is given in Fig. 1. The experimental setup is shown in Fig. 2a, which includes a Styrofoam base that contains a curved depression into which the syringe can be placed during classification. The Styrofoam base helps to firmly immobilize the syringe during measurement and was designed to increase the accuracy and precision of the system.

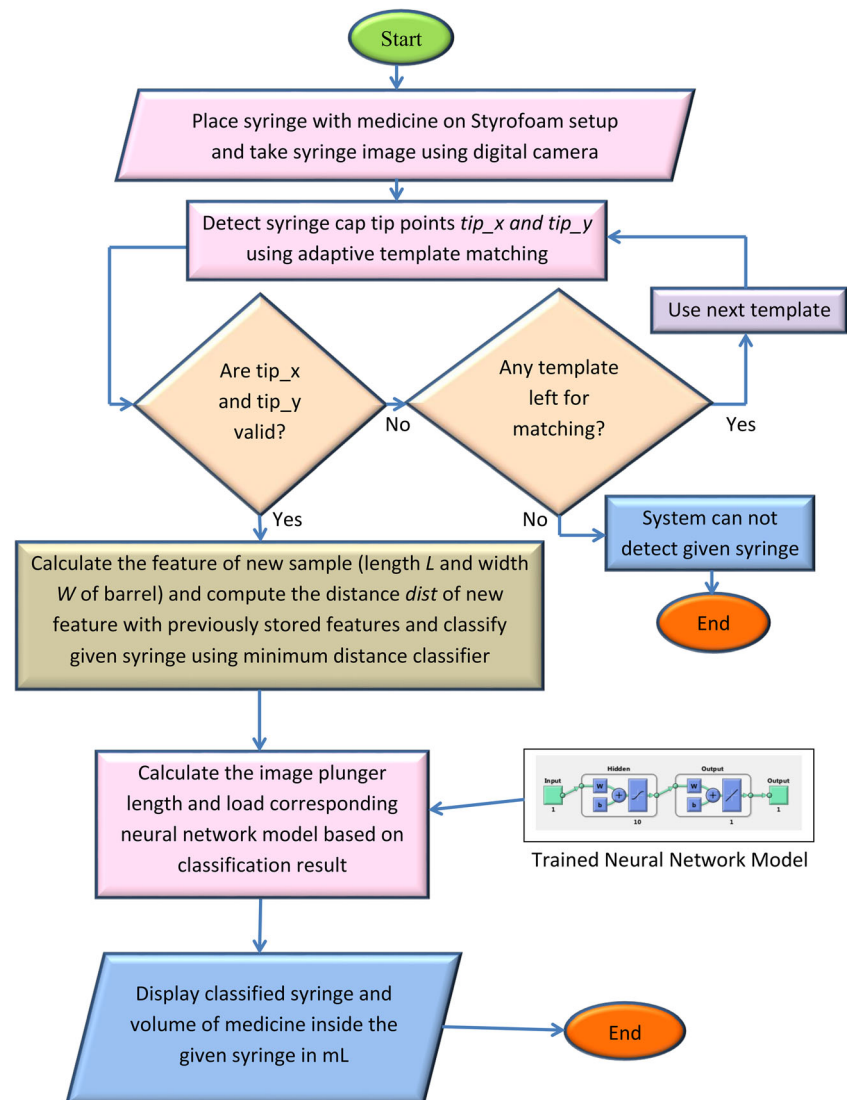
Image Acquisition and Pre-processing

The configuration of the system and its components was set up to work in real-time. A Logitech webcam (Model C615) digital camera was interfaced with a PC. A MATLAB program was developed that uses a special routine to start the digital camera and video and image acquisition. For the purposes of this initial project, the digital camera was fixed at an appropriate height from the surface of a Styrofoam base holding the syringe as shown in Fig. 2a. Real-time video input obtained from the digital camera was supplied to the MATLAB program, which extracted images from the various frames of the video feed. Images obtained by the camera were enhanced using histogram equalization to balance intensity and median filtering was utilized to remove noise. A histogram equalization of the image with 64 different levels was employed to derive an image with a uniform intensity distribution. Median filtering with a window of size 3×3 was applied to remove small dots present in the syringe and background. The aforementioned digital image processing completed within the MATLAB program rendered the image suitable for segmentation.

Syringe Classification System

The syringe classification system (SCS) proceeds to detect the correct syringe size through several sub-routines occurring sequentially starting with detection of the syringe tip cap via template matching, followed by whole syringe image processing using image acquisition and pre-processing (IAPP), and ending with syringe width and length calculations. To enable identification of the proper syringe tip cap, several template images of syringe tip caps of various colors placed in a variety of spatial orientations were stored by creating a database. Figure 2c, d shows representative templates of blue and yellow colored syringe tip caps that were used in the experiments. Individual template images have a size of 150×200 and the whole image had a size of 1080×1920 . The template matching technique determines the perfect match point location in the target image whose

Fig. 1 Flow chart of complete system (syringe classification and volume measurement)



appearances match one of the template images stored in the database. The developed MATLAB program receives the image frame obtained from the digital camera and loads various templates of blue and yellow syringe tip caps. One unique template image from the database is run over the entire target image (e.g., whole image of syringe) to find the best match point in the target image. The template-sized portion of the target image is extracted from the target image, and cross-correlation is computed with template image using Eq. 1 [23, 24].

$$\eta = \frac{\sum_{i,j \in W} I1(i,j) \cdot I2(x+i, y+j)}{\sqrt{\sum_{i,j \in W} I1^2(i,j)} \cdot \sqrt{\sum_{i,j \in W} I2^2(x+i, y+j)}} \quad (1)$$

In Eq. (1), η is the normalized correlation coefficient and $I_i(x,y)$ is the intensity value at position (x,y) . After the syringe tip cap detection was completed, the whole syringe image was processed to enhance the image via

IAPP. The enhanced image was then subjected to segmentation, and the barrel width calculation process started using connected region analysis [28]. The connected region analysis gives the area, length, and width properties of the sub-regions of the whole binary image, as shown in the Fig. 4b. The detected syringe tip cap from the first part of this process is an important attribute utilized for classification and barrel length calculation. After the volume measurement system (VMS) detected the syringe tip cap, its centroid was computed. In order to compute the centroid of the black rubber tip of the plunger, the grayscale image of the syringe was subjected to segmentation after the IAPP process. After segmentation, the binary image was obtained, as shown in Fig. 4b. Following this, the eight-connected analysis was applied in the binary image, and the largest continuous region was extracted and separated from the original binary image as shown in Fig. 4c. This image, representing the syringe space between the

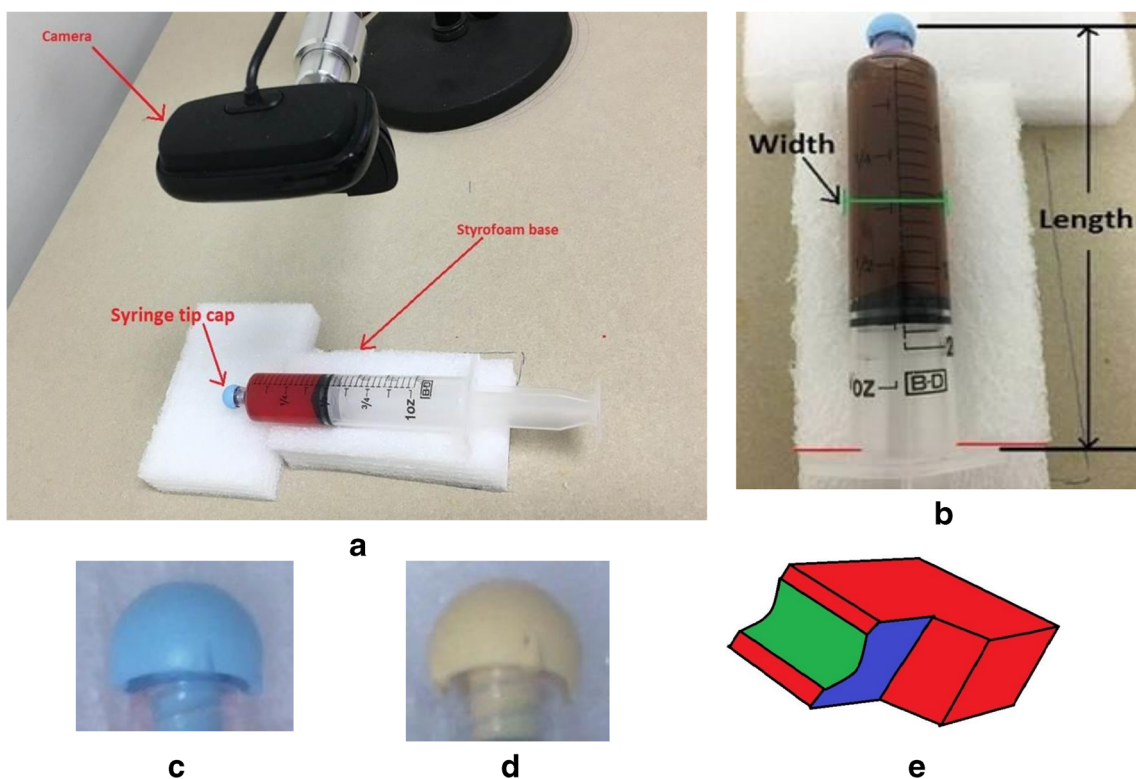


Fig. 2 a Experimental setup of the system; b plan view of syringe on Styrofoam base showing barrel length and width; c template of blue syringe tip cap; d template of yellow syringe tip cap; and e layout of Styrofoam base

syringe tip cap and the plunger region, was first eroded and then dilated to remove noise on the edges. Equation 2 shows how the distance *dist* was determined.

$$dist = |S - M_i| \tag{2}$$

Where, $S = \{L, W\}$, L = syringe length, W = syringe barrel width, and M_i = mean feature vector of syringes of various sizes, $i = 1$ to 6. The mean feature vector of each syringe was computed from 50 previously recorded data vectors.

The *dist* vector represents the difference between the mean feature vector of a new sample image of the test syringe and the mean feature vector point of six syringes considered in classification. A zero or near zero value of the *dist* vector indicates a perfect match between the new sample image and the syringe size corresponding to the mean feature vector point in the previously recorded data. Thus, a feature vector comprised two features, namely the syringe length and syringe barrel width, that were used to conclusively classify and assign the size of a particular test syringe. The Luer-lock syringes tested had plungers that have a black, latex-free rubber tips and the yellow and blue syringe tip caps were made of thermoplastic elastomers. Clear tap water and aqueous solutions of yellow-, red-, and blue-colored dye were used to simulate medication in the syringe.

Volume Measurement System

The second component of the system comprises features that support the automated measurement of the volume of medication contained inside a syringe. The volume of medication measured inside the syringe primarily relies on the plunger depth (PD) calculation, and this process is demonstrated in Fig. 4. PD is defined as the length between the centroid of the syringe tip cap located in the upper region of the syringe and the centroid of the black rubber tip of the plunger located in the lower barrel region of the syringe. In Fig. 4e, the green dot marks the syringe tip cap centroid and the red dot marks the plunger tip centroid. Both the digital camera and the Styrofoam base are fixed at a particular position so when the syringe containing the medication is placed on the base the orientation of the syringe is such that the syringe tip cap will always be on the top of the acquired image and the plunger rubber tip will be towards the bottom. The VMS detects the syringe tip cap, and calculates the syringe tip cap and plunger rubber tip centroids after processing the image as described under SCS. The volume of medication taken inside the syringe was manually filled and adjusted to various volume markings by withdrawing the syringe plunger then fed into the MATLAB program for PD calculation when the VMS was trained. The MATLAB program calculated the PD using the procedure described above. The calculated PD and

corresponding actual liquid volume makes a data pair, and several data pairs were generated and stored in a Microsoft Excel spreadsheet, as shown in Fig. 6, to create a database. An identical procedure was followed for all six syringe sizes when creating the expanded database. The database contained 500 data pairs for each syringe size in six separate data files. The developed database was utilized to train an ANN composed of 10 hidden neurons, one input and one output. From the database, the plunger depth was used as the input and the observed volume was the output for training. At the conclusion of training, there were six trained neural network models for each syringe size that takes plunger depth as input and gives the volume of medication inside the syringe as the output.

After the syringe classification process gave the result in string, the text was compared with a previously stored array of text,

$$\text{Array} = \{ \text{'One'}, \text{'Three'}, \text{'Five'}, \text{'Ten'}, \text{'Twenty'}, \text{'Thirty'} \}$$

When the result string matched with one of the six strings in the array, the corresponding trained neural network model gets called and the plunger depth passed to the model. Subsequently, the volume of medication inside the syringe is obtained as the output.

Results and Discussion

The syringes used in the experiments were commercially available Luer-lock syringes, which are used during aseptic compounding of sterile preparations and for packaging parenteral preparations in the form of prefilled syringes. The experimental setup can be reproduced, configured, and implemented effortlessly and with minimal cost in pharmaceutical laboratories, compounding pharmacies, or pharmaceutical industry. The entire system was developed in MATLAB R2013a utilizing the neural network training and image processing toolboxes. With a single acquisition of an image frame from video, the system accurately and precisely classified the type of syringe utilized and the volume of medication contained inside in real time. The system is versatile enough to classify and measure syringe volume even when the syringe contains colored medication.

Syringe Classification System

The system performed syringe classification without any error. A high success rate is required during the syringe classification step, because the subsequent volume measurement relies on proper syringe classification. This is because the obtained syringe classification result decides which trained neural network model gets loaded to map the calculated

plunger depth into the volume of medication. The template matching technique then determines the perfect match point by performing correlation calculations based on Eq. 1. This calculation process progresses from the left-top point row by row to the right-bottom point of the target image and correlation coefficients were stored in a 2D matrix. Thus, when the calculation process is complete, the largest value with its index (pixel location) obtained from the 2D matrix provides the best match between the template image and the target image. If a match point is not detected in the first trial with one colored syringe tip cap, then another colored template is loaded and the process repeated again to locate the best match point. To enable optimal detection of the best match point, some experimental setup constraints were imposed. One such constraint was the limit of the region of interest during the detection of the syringe tip cap. In the experimental setup, the detection points were set between 150 and 700 for vertical length of image. These points were set based on the initial experimental readings taken as the system was being developed. Thus, if the detected points in the target image do not fall within this criteria then other template images are loaded, and the whole process is run again until it gives the matching valid detected points. One drawback of this type of constraint is that this could lead to an increase in system computation time. Another constraint was that the lower end of the syringe barrel was locked in the Styrofoam as shown in Fig. 2b, and that point is always constant in the image since the camera is immobile and attached at a point in a metallic stand. The calculated barrel length is the distance between the lower end of the syringe barrel and syringe tip cap point. As shown in Fig. 2b, the red horizontal line indicates the distance between the blue colored syringe tip cap and the lower end point of the syringe barrel. The barrel width is indicated by the green horizontal line in Fig. 2b. Figure 2e shows the schematic diagram of the Styrofoam base that was used to hold the syringes during testing and is colored in the diagram to describe its functionality. The green-colored surface indicates the concavity introduced by cutting the Styrofoam so that it holds the syringe without any movement when placed. The blue-colored side is a cut surface that meets the green concavity to form an edge and helps to hold the syringe barrel flange in position when measurements are made.

When the connected region analysis was done following image segmentation, only a single binary connected region with the largest area in the image was selected, and all other smaller regions were removed, because this portion of the syringe with or without medication always yielded the largest region in the segmented binary image. Barrel length (L) is a strong feature during syringe classification because 30, 20, 10, and 1 ml syringes could be easily identified due to their inherent differences in length. However, 5 and 3 ml syringes possessed similar barrel length. Thus, barrel width (W) was also taken into consideration to make the classification more robust

and efficient. The width of the largest connected region is the barrel width as shown in Fig. 4c.

In Fig. 3, the cluster of data points of six different size syringes is shown with the corresponding mean feature vector point (see figure legend). There is a small scatter associated with the 50 samples from each syringe size shown in six separate clusters that were used to compute the mean feature vector point for each syringe. The narrow clustering of the data points seen in the results indicates the flawless performance of the syringe classification step. Additionally, the low spread of the mean feature vector points denotes the high accuracy and precision of the system. There is adequate distance between the data clusters of different syringes which is key to making an error-free syringe classification. Figure 3 distinctly shows that based on the barrel length (major feature) and the barrel width (minor feature) the six syringe sizes used during compounding can be easily classified. The mean feature vector points of each syringe are shown in solid colors or solid colors with a dot in the middle. The length shown in the X-axis in Fig. 3 is the barrel length in pixels. The result from the syringe classification stage was obtained as a string indicating one of the six syringe sizes utilized during testing. The efficiency of the system to classify the syringe was tested and found to be errorless during all trials for each syringe size. During these trials, the plunger was withdrawn to various volume markings in a particular syringe. This was done to simulate actual situations under which the syringes are typically used when preparing or dispensing a compounded sterile

preparation. As an example, for the 30-ml syringe (Fig. 4a), the syringe classification process was tested by changing the plunger position by 1 ml starting at 30, 29, 28 ml, down to 1 ml. Similarly, 20, 10, 5, 3, and 1 ml syringes were tested with plunger positions varied according to the syringe capacity. Representative pictures of syringes and plunger positions used during classification are shown in Fig. 5. Figure 5a–f shows the classification output string in the lavender-colored box titled “Syringe Classified.” The original image of various syringes with the plunger at different positions is also shown as follows: for 30 ml syringe plunger position at 18 ml, 20 ml syringe plunger position at 13 ml, 10 ml syringe plunger position at 4 ml, 5 ml syringe plunger position at 3 ml, 3 ml syringe plunger position at 1.3 ml, and 1 ml syringe plunger position at 0.6 ml respectively.

Volume Measurement System

A critical step during the volume measurement process is determination of the plunger depth starting with image segmentation, calculation of the syringe tip cap and plunger rubber tip centroids, and calculation of the vertical distance between the syringe tip cap centroid and the plunger rubber tip centroid. A sufficiently large threshold value was used during image segmentation to clearly separate the background image and foreground object. An important goal of the image segmentation process was to preserve the black rubber tip region of the syringe plunger. The threshold value used allowed that only

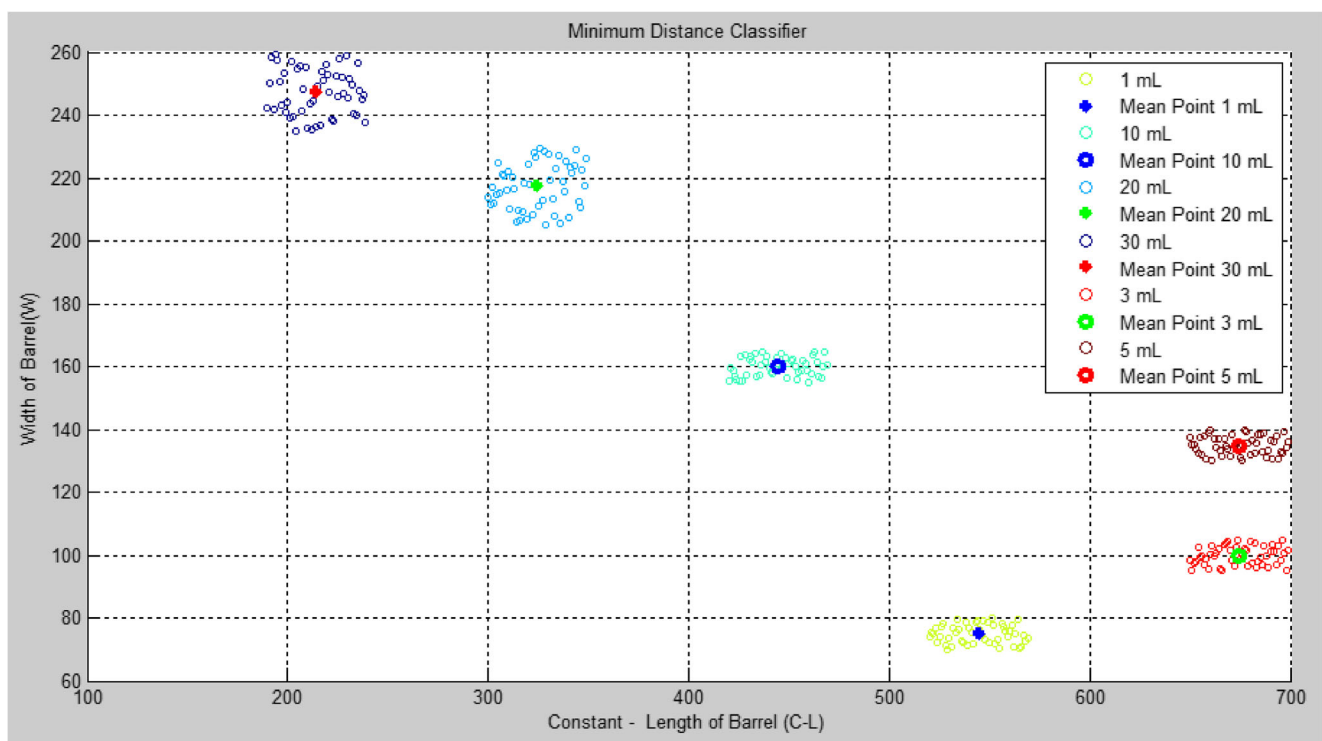


Fig. 3 Data points and mean point plot for minimum distance classifier

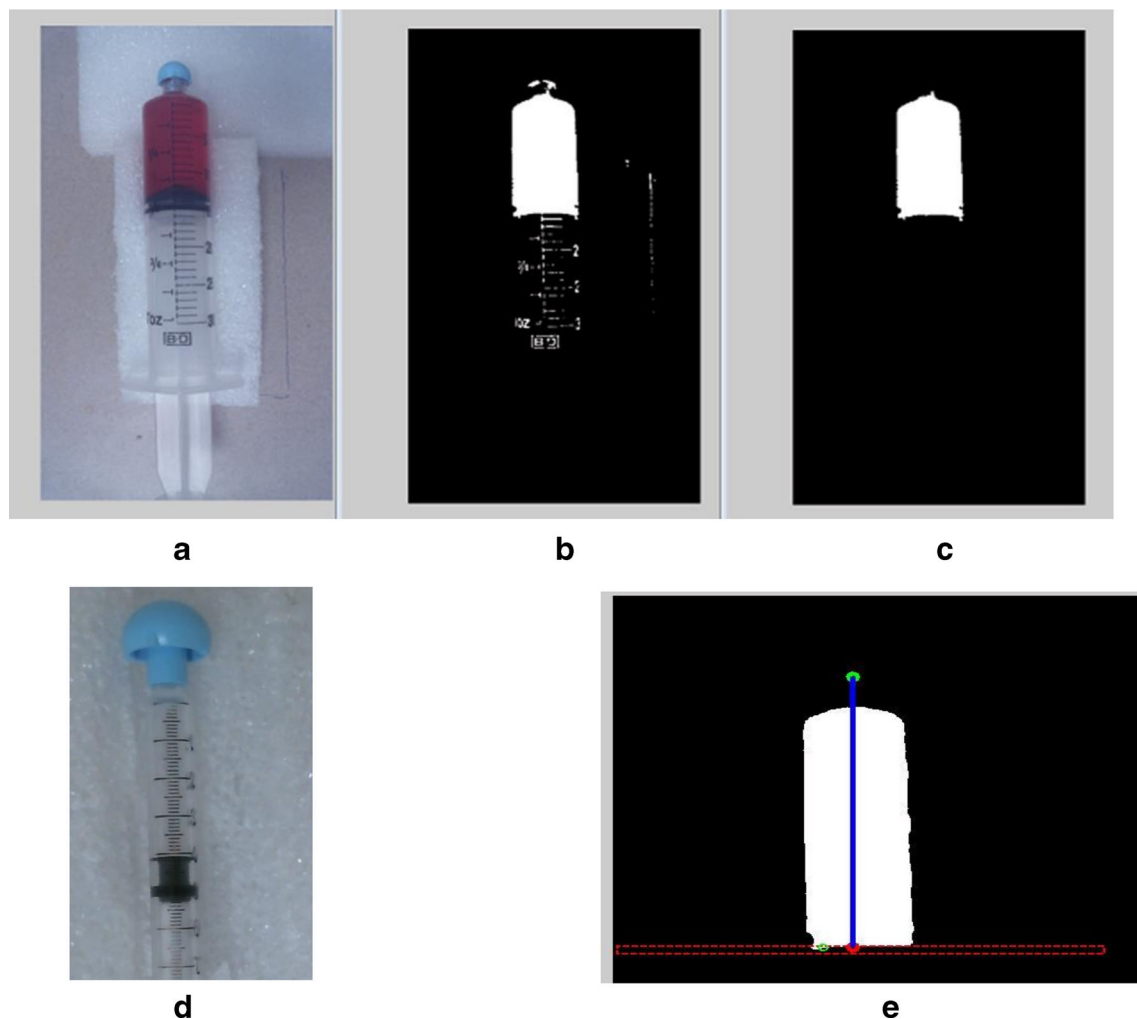


Fig. 4 Screenshots of **a** original image of 30 ml syringe with colored medication; **b** binary output image; **c** largest connected region of binary image; **d** original image of 1 ml syringe with colorless medication; **e** plunger length calculation

regions with very low intensity be retained even though absolute segmentation was not necessary. Since the plunger region in the extracted image was always at the bottom part of the image according to the experimental setup, the lowest 200 pixels from the image were taken into account and the centroid calculated as shown in Fig. 4e. The rectangular window lined by red dashes shows the region containing the lowest 200 pixels, and the green dot is the calculated centroid. This process helped obtain an accurate and precise value of the reference point for the plunger region in each experiment and minimized the dependency of the calculated centroid to the thresholding technique. In order to make the image length consistent and to minimize error associated with thresholding during each experiment, only the vertical distance was taken into consideration, which means that the difference between x-coordinates was neglected. The difference between the y-coordinates of the syringe tip cap centroid and the centroid of the plunger region gave the plunger depth. The plunger depth at this stage was fed as input in the neural network model for

the particular syringe size that followed the syringe classification stage. The neural network model then noted the plunger depth and gave the corresponding volume of medication as the output.

A portion of the dataset for 5 and 10 ml syringes is shown in Fig. 6a, b. The dataset contains the plunger depth in the left column labeled A and the corresponding actual volume of medication in the right column labeled B. For the 5-ml syringe, the system has a scale resolution of 0.2 ml which is the minimum amount of liquid that can be accurately measured using this syringe. Since the 5-ml syringe had volume level markings in 0.2 ml increments, the dataset for 5 ml syringe were collected by keeping the plunger position at every possible volume marking on the syringe from 0.2 to 5 ml producing a total of 25 data pairs. Multiple data pairs were collected at one particular plunger position to collect and expand the database for use during neural network training. Each image captured of the same syringe size may appear similar to a previous image of the

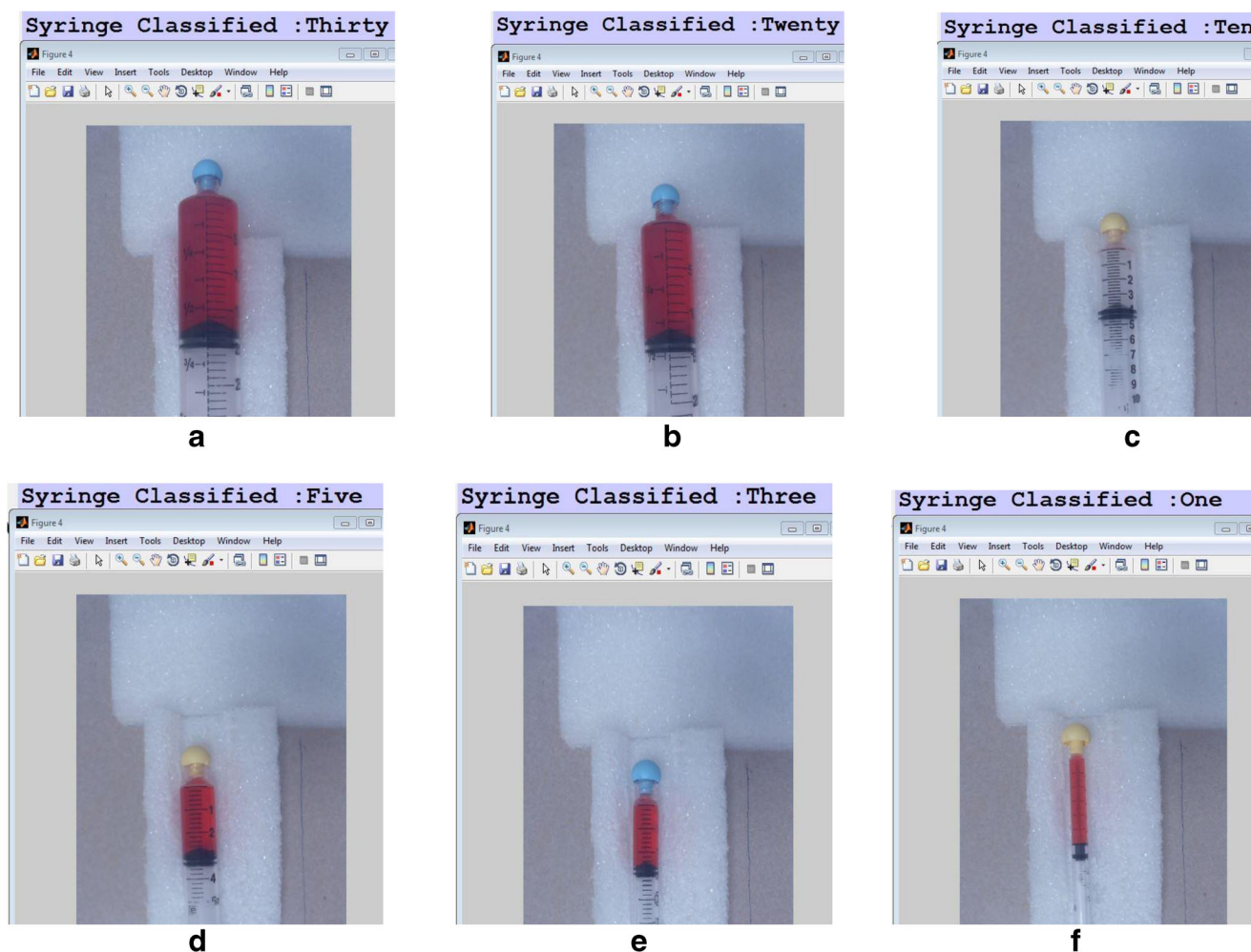


Fig. 5 Screenshots of syringe classification stage output **a** 30 ml; **b** 20 ml; **c** 10 ml; **d** 5 ml; **e** 3 ml; and **f** 1 ml

same syringe, but the syringe may be slightly tilted or removed from the Styrofoam base and replaced back again or slightly moved from its original position before a new image was captured. This was performed to account for small changes in the orientation of the syringe when it is placed before a volume reading was done during data collection. By this method, a total of 500 samples were collected for each syringe, and the artificial neural network model was trained for all syringes, and the trained model was utilized during volume measurement.

Figure 6d–f shows the neural network training of a 10-ml syringe. The ANN was trained using the Levenberg-Marquardt backpropagation method [35]. In Fig. 6d, the green asterisks were the output points obtained after the network was trained, while blue circles indicate the targeted output points. Thus, the deviation of green asterisk from blue circles indicates the margin of error, and as the figure illustrates the green asterisks are superimposed on the blue circles indicating that there is minimal error associated with the neural network model. The ANN performance was measured in mean squared error (MSE) as

shown in Fig. 6e where the graph demonstrates that the error diminished to approximately 0.001 by 39 epochs. The whole sample dataset was divided into training data, validation data, and test data. The validation curve (green line) indicates the response of the neural network model to the data that was used to define the stopping criteria of the training process. The test curve (red line) was used to test the overfitting and under-fitting of data to the neural network model. The training error curve (blue line) is the response obtained from the neural network to the data that were used for training only. The trends in the graphs show that MSE was large at the beginning while it decreased sharply after a few epochs and finally became constant indicating when the training came to completion. The training curve is lower than validation curve and test curve indicating that training error was always minimal. Generally, in the training process, about 70–80% of the samples are used for training, approximately 15% for validation and the remaining for testing. Thus, the training data are specifically used to build the mathematical model during training process. The validation data are used to

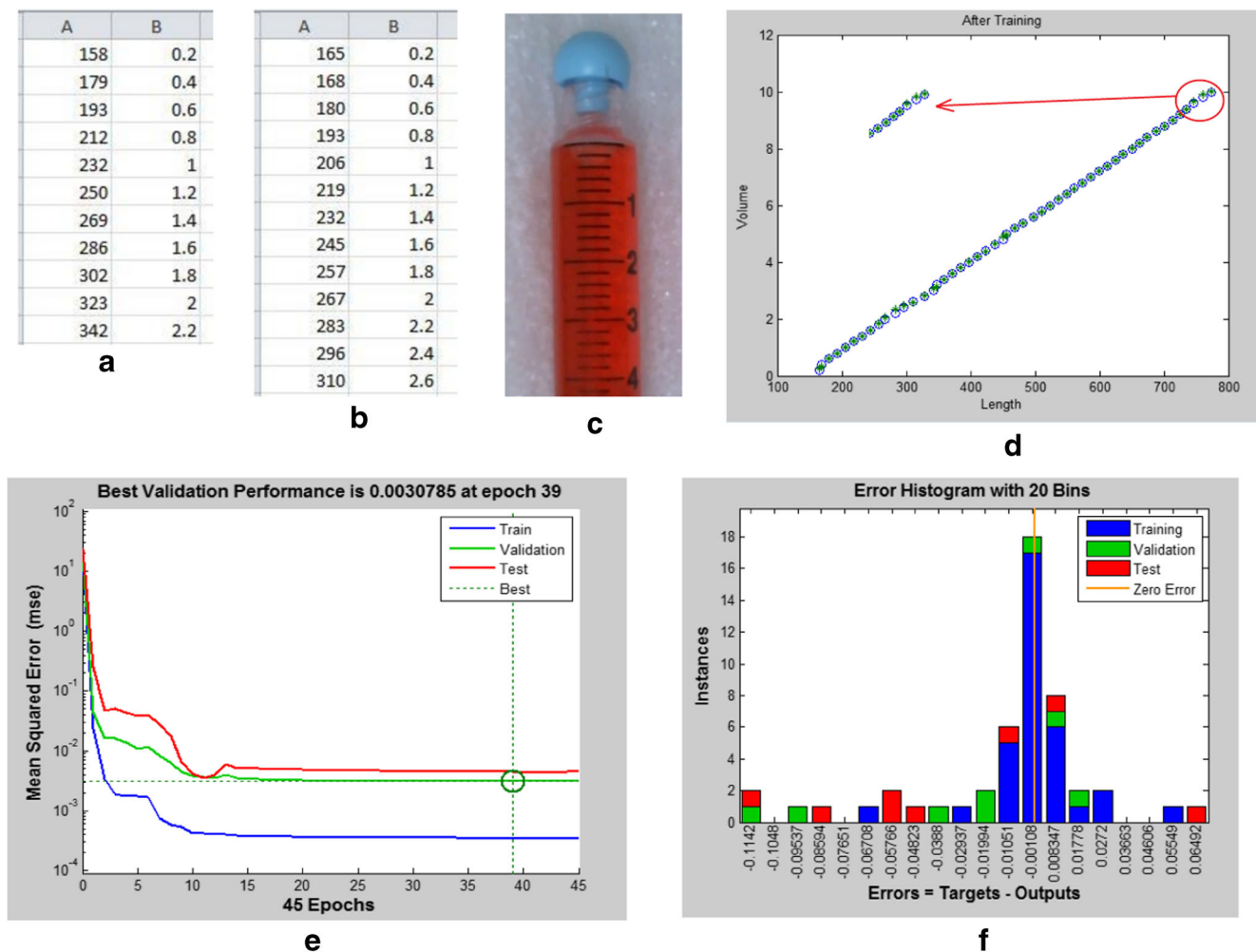


Fig. 6 Screenshots of **a** 5 ml dataset; **b** 10 ml dataset; **c** 5 ml zoomed image; **d** input/output plot for 10 ml after training; **e** training, validation, and test errors plotted against MSE for 10 ml; **f** error histogram diagram for 10 ml

calculate the error to determine the termination condition of the training process. The testing error should be close to validation error for successful completion of training. The validation and test curves in this work were very similar indicating that the training process was successfully completed. Figure 6f shows the error histogram with instances of test in Y-axis and errors associated with each instance in the X-axis. The histogram indicates that during training, test, and validation, most instances of the error were around the value of 0.00108 which corresponds to the plateau observed in the curve (Fig. 6e) of training, validating, and testing. The yellow vertical line in the histogram signifies that positive and negative errors eventually converged towards minimum error, and the greatest number of instances (Y-axis entity) have nearly zero error.

Since an error-free syringe classification result was required for volume measurement, the performance of volume measurement was evaluated in conjunction with syringe classification with various syringe sizes. Experiments were performed with all syringe sizes using assorted plunger positions,

and the volume obtained from the system was documented along with computation time. Further, for any particular syringe size, the complete system was tested with different combinations of syringe tip caps and medication color. It may be noted that when using a syringe ideally, a volume less than one third of its total capacity or a volume exceeding two thirds of its total capacity may not be taken in it. The developed system was evaluated at a range of volumes throughout the capacity of tested syringes as a measure of robustness of the system. The performances of various syringes analyzed separately to determine the accuracy, precision, and best working range are described below.

Thirty Milliliters

To test the accuracy and precision, trials were performed using different volumes of medication inside the syringe for all four aforementioned colored medications and two syringe tip caps. Table 1 shows the performance of the 30-ml syringe when 5, 15, 20, 25, and 30 ml of simulated medication were taken in

Table 1 Observed volume, computation time and accuracy for 30 ml syringe with yellow-colored medicine

Syringe size (max. capacity)	Volume in syringe (ml)	Detected volume (ml)	Detection time (s)	Mean \pm SD	Accuracy (%)
Syringe: 30 ml	Medicine: yellow			Syringe tip cap: blue	
30 ml	5.0	5.3418	7.4689	5.3187 \pm 0.0200	93.62
		5.3065	7.5848		
		5.3079	7.4982		
	15.0	15.4268	7.362	15.4125 \pm 0.0236	97.25
		15.4254	7.3354		
		15.3853	7.3467		
	20.0	19.9458	7.4724	19.9420 \pm 0.0270	99.71
		19.9669	7.4817		
		19.9133	7.4541		
	25.0	24.9481	7.3549	24.9499 \pm 0.0017	99.79
		24.951	7.4219		
		24.9505	7.3674		
	30.0	30.0299	7.4582	30.0271 \pm 0.0024	99.90
		30.0257	7.4806		
		30.0257	7.4731		
Syringe: 30 ml	Medicine: yellow			Syringe tip cap: yellow	
30 ml	5.0	5.3562	5.6312	5.3484 \pm 0.0275	90.03
		5.3712	5.6762		
		5.3179	5.6816		
	15.0	15.2695	5.5527	15.3023 \pm 0.0284	97.98
		15.3184	5.5211		
		15.3189	5.5512		
	20.0	19.962	5.632	19.9418 \pm 0.0349	99.70
		19.962	5.6373		
		19.9015	5.6976		
	25.0	24.8936	5.5793	24.8931 \pm 0.0005	99.57
		24.8933	5.5518		
		24.8925	5.558		
	30.0	29.9949	5.6234	29.9952 \pm 0.0003	99.98
		29.995	5.636		
		29.9956	5.7721		

the syringe. The experiments were done in triplicate and the data shown is for yellow-colored medication using yellow- and blue-colored syringe tip caps to seal the syringe. An accuracy of 97 to 99% was seen for volume range from 15 to 30 ml suggesting that this is the best working range for 30 ml syringe. The observed standard deviation during the trials ranged from 0.0003 to 0.0349 showing high precision of the system. The 30-ml syringe had a resolution of 1 ml, so it can only be practically utilized to measure volumes differing by 1 ml when the measured volume is manually checked through visual inspection. The system reported in this manuscript can precisely detect correct volumes with a resolution less than 1 ml as illustrated in Fig. 7a. In this figure, based on the plunger position used during the experiment, it is not possible to discern the exact volume by manually inspecting the plunger position since the syringe does not have volume markings between 15 and 16 ml printed on the syringe. However, the

system gave the volume measured accurately as 15.24 ml based on the trained ANN model.

Twenty Milliliters

Table 2 shows the results obtained during testing of 20 ml syringe capped with yellow and blue syringe tip caps containing red colored medication. The 20-ml syringe had a resolution of 1 ml; thus, the volume markings printed on the syringe were from 1 to 20 ml. Experiments were performed with 1, 5, 10, 15, and 20 ml of simulated medication in the syringe. Accuracy was approximately 69% in the presence of red medication and yellow syringe tip cap while it was 76% in the presence of red medication and blue syringe tip cap when 1 ml medication was present in the syringe. The accuracy increased to between 96 and 99% when volumes from 5 up to 20 ml were measured indicating that this was the best

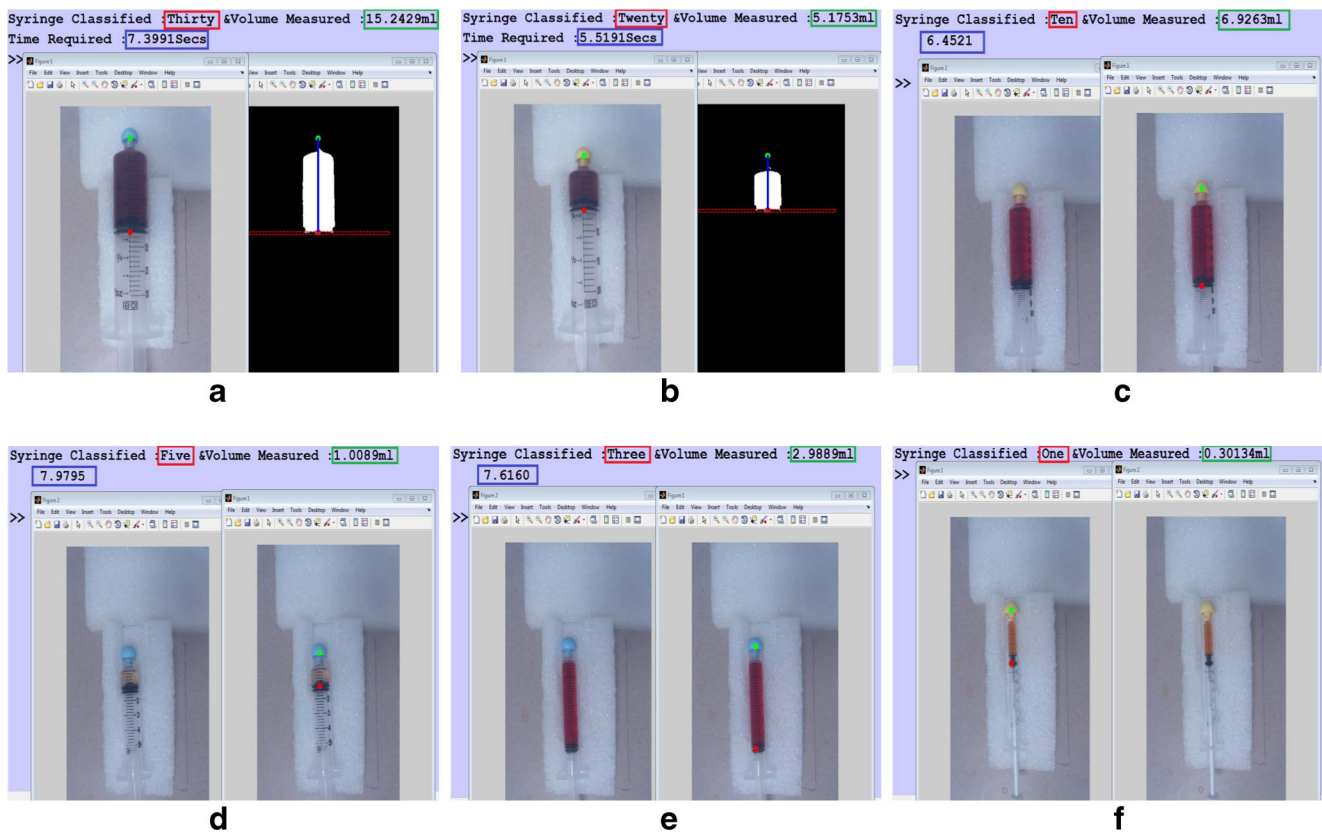


Fig. 7 Screenshot of complete system output showing syringe type, volume measured, and computational time for **a** 30 ml; **b** 20 ml; **c** 10 ml; **d** 5 ml; **e** 3 ml; and **f** 1 ml

working range for the 20-ml syringe. The standard deviation in the volume range 5 to 20 ml was 0.0080–0.0057 which indicated the high precision of the system. The computer screen output when testing the 20-ml syringe containing 5 ml liquid is shown in Fig. 7b. The image shows the classified syringe output in red box, volume measured in green box, and computational time required in blue box.

Ten Milliliters

The 10-ml syringe had a resolution of 0.2 ml and trials were performed using 1.0, 3.0, 5.0, 7.0, and 9.0 ml of medication in the syringe. The results obtained when red-colored simulated medication was used along with yellow and blue syringe tip caps are shown in Table 3. From 3.0 to 9.0 ml, accuracy was observed to be consistently between 97 and 99% suggesting that this was potentially the best working range for the 10-ml syringe. The standard deviation was found to be between 0.0017 and 0.0205 when 3 to 9 ml volumes were measured and consequently shows the high level of precision obtained in that volume range. When volumes from 1 ml down to 0.2 ml were measured in this syringe, the trial results demonstrated very low accuracy (data not shown). The screen output of the system when the 20-ml syringe was used to measure 7 ml liquid volume is shown in Fig. 7c.

Five Milliliters

The system was tested with medications of 1, 2, 3, 4, and 5 ml volumes and using all colors and syringe tip caps. The observed data is shown in Table 4. The 5-ml syringe had a resolution of 0.2 ml and results show that it performed optimally from 1.0 to 5.0 ml with an accuracy of 97 to 99% and with a level of precision between 0.0002 and 0.0154. The accuracy decreased to less than 85% below 1 ml volume and continuously decreased until the minimum measurable volume of 0.2 ml. Thus, the best working range for the 5 ml syringe was found to be from 1 to 5 ml. The screen output of the system for the 5-ml syringe when used to measure 1 ml liquid volume is shown in Fig. 7d. It shows the classified syringe output, volume measured, and computational time required for this particular setup in red, green, and blue rectangular windows, respectively.

Three Milliliters

The 3-ml syringe had a resolution of 0.1 ml. The trained model built from previously collected data was used to test the performance of the system when the liquid volume in the syringe was 0.5, 1.0, 1.8, 2.5, and 3.0 ml. The accuracy of the system in the volume range of 1.0 to 3.0 ml was between

Table 2 Observed volume, computation time, and accuracy for 20 ml syringe with red-colored medicine

Syringe size (max. capacity)	Volume in syringe (ml)	Detected volume (ml)	Detection time (s)	Mean \pm SD	Accuracy (%)		
Syringe: 20 ml		Medicine: red		Syringe tip cap: blue			
20 ml	1.0	0.7925	7.3815	0.7591 \pm 0.0592	75.91		
		0.7942	7.3619				
		0.6908	7.3482				
	5.0	5.1762	7.3206			5.1750 \pm 0.0022	96.50
		5.1763	7.3191				
		5.1724	7.3958				
	10.0	10.0304	7.3306			10.0292 \pm 0.0017	99.70
		10.0299	7.3697				
		10.0272	7.3403				
	15.0	14.4481	7.3311			14.4475 \pm 0.0008	96.31
		14.4478	7.3296				
		14.4466	7.3554				
	20.0	19.6253	7.8535			19.6252 \pm 0.0008	98.12
		19.6244	7.6066				
		19.6260	7.6212				
Syringe: 20 ml		Medicine: red		Syringe tip cap: yellow			
20 ml	1.0	0.6962	5.5965	0.6910 \pm 0.0053	69.10		
		0.6913	5.5478				
		0.6855	5.6518				
	5.0	5.1644	5.5303			5.1629 \pm 0.0023	96.74
		5.1641	5.5351				
		5.1603	5.5443				
	10.0	9.9590	5.4774			9.9584 \pm 0.0008	99.58
		9.9586	5.5399				
		9.9575	5.5541				
	15.0	14.4526	5.5078			14.4559 \pm 0.0057	96.37
		14.4526	5.4474				
		14.4624	5.5711				
	20.0	19.6275	5.8215			19.6243 \pm 0.0028	98.12
		19.6224	5.8093				
		19.623	5.8065				

97 and 99% as shown in Table 5. The observed standard deviation, which indicates the accuracy in the same volume range, was between 0.0001 and 0.0016. The accuracy decreased to approximately 90% when the liquid volume in the syringe was 0.5 ml. The screen output of the system for the 3-ml syringe when used to measure 3 ml volume is shown in Fig. 7e.

One Milliliter

The 1-ml syringe had the capacity to measure from 0.01 to 1 ml volumes. The trained model for 1 ml syringe was tested above 0.05 ml because the plunger was indistinguishable from syringe tip cap below the setting of 0.05 ml because of the small size and narrow diameter of the syringe barrel. Trials were performed with 0.05, 0.25, 0.5, 0.75, and 1.0 ml of simulated medication and using yellow and blue syringe tip caps.

The observed volumes with accuracy and precision are shown in Table 6. The results show that the best working range for 1 ml syringe was from 0.25 to 1.0 ml with accuracy between 96 and 99% and standard deviation from 0.0001 to 0.0106. From 0.05 to 0.25 ml, accuracy was found to be between 85 and 95% (data not shown). The screen output of the system the 1-ml syringe was used to measure 0.3 ml volume is shown in Fig. 7f.

Apart from the particular medication and syringe tip cap described above under each individual syringe size above, trials were performed using all other colored medications and syringe tip caps listed in the methods section with similar results, accuracy, and precision (data not shown).

In all the observations, the syringe length and corresponding volume that are the input and output data showed a linear relationship. This is primarily attributed to the algorithm used for plunger length calculation. The algorithm mostly relies on

Table 3 Observed volume, computation time, and accuracy for 10 ml syringe with red colored medicine

Syringe size (max. capacity)	Volume in syringe (ml)	Detected volume (ml)	Detection time (s)	Mean ± SD	Accuracy (%)		
Syringe: 10 ml 10 ml	Medicine: red 1.0	0.9948	7.4828	Syringe tip cap: blue 0.9902 ± 0.005	99.02		
		0.9850	7.5208				
		0.9910	7.9006				
	3.0	2.9608	7.5178			2.9600 ± 0.0017	98.66
		2.9580	7.5647				
		2.9612	7.6656				
	5.0	4.9548	7.6990			4.9311 ± 0.0205	98.62
		4.9187	7.6696				
		4.9198	7.7008				
	7.0	6.9310	7.7449			6.9309 ± 0.0004	99.01
		6.9305	7.7054				
		6.9313	7.7083				
	9.0	8.9791	7.3654			8.9792 ± 0.0002	99.76
		8.9794	7.5265				
		8.9790	7.3247				
Syringe: 10 ml 10 ml	Medicine: red 1.0	1.0522	6.5983	Syringe tip cap: yellow 1.0484 ± 0.0033	95.16		
		1.0470	5.7334				
		1.0460	5.6968				
	3.0	3.0943	5.6405			3.0908 ± 0.0034	96.97
		3.0876	5.6361				
		3.0904	5.9507				
	5.0	5.0086	5.7396			5.0052 ± 0.0078	99.89
		5.0107	5.7583				
		4.9963	5.7499				
	7.0	6.9562	5.6114			6.9701 ± 0.0121	99.57
		6.9763	5.5938				
		6.9779	5.5824				
	9.0	9.0567	5.3859			9.0625 ± 0.0094	99.30
		9.0574	5.5616				
		9.0733	5.5958				

the position of the black-colored rubber plunger and little to no weightage is provided for the color of the liquid inside the syringe making the system robust. The plunger depth, and hence the length of medication in a particular syringe, is directly correlated to the volume of medication present and that is effortlessly established by the trained artificial neural network model.

Volume Measurement Using Linear Model

During the experiments using all the datasets developed for the neural network model, one trend that was seen was that with the exception of few data points all syringes had near linear input-output relationship. Thus, as the ANN was being trained, simultaneously the system was tested using a linear model and results were obtained. The linear model was built using only three points from the dataset: initial point (x_0, y_0),

mid-point (x_m, y_m), and final point (x_f, y_f). For example, in the 5-ml syringe, the plunger depth and volume pair (158, 0.2) at 0.2 ml was taken as the initial point, pair (377, 2.6) at 2.6 ml was the middle point, and the pair (596, 5.0) at 5 ml was the final point. Then if x represents the plunger depth obtained from the analysis, then y which is the volume of medication contained in the syringe was calculated using the equation below.

$$y = \frac{y_m - y_0}{x_m - x_0} \times (x - x_0) + y_0 \text{ if } x < x_m$$

and

$$y = \frac{y_f - y_m}{x_f - x_m} \times (x - x_m) + y_m \text{ if } x \geq x_m$$

This method was tested for all the data pair combinations as described under neural network training (data not shown). The

Table 4 Observed volume, computation time and accuracy for 5 ml syringe with water

Syringe size (max. capacity)	Volume in syringe (ml)	Detected volume (ml)	Detection time (s)	Mean ± SD	Accuracy (%)		
Syringe: 5 ml		Medicine: water		Syringe tip cap: blue			
5 ml	1.0	0.9687	7.5453	0.9690 ± 0.0004	96.90		
		0.9690	7.5387				
		0.9694	7.5476				
	2.0	2.0809	7.4915			2.0828 ± 0.0041	95.86
		2.0799	7.5207				
		2.0875	7.5747				
	3.0	2.9372	7.6427			2.9364 ± 0.0009	97.88
		2.9364	7.5619				
		2.9355	7.5365				
	4.0	3.9848	7.4891			3.9902 ± 0.0099	99.75
		3.9842	7.5646				
		4.0017	7.5337				
	5.0	4.9208	7.5161			4.9200 ± 0.0007	98.40
		4.9196	7.5392				
		4.9196	7.5670				
Syringe: 5 ml		Medicine: water		Syringe tip cap: yellow			
5 ml	1.0	1.0000	5.5497	0.9999 ± 0.0002	99.99		
		0.9997	5.5721				
		1.0001	5.6118				
	2.0	2.0963	5.5457			2.0965 ± 0.0002	95.17
		2.0967	5.5563				
		2.0966	5.5432				
	3.0	2.9929	5.6084			2.9922 ± 0.0008	99.74
		2.9913	5.5610				
		2.9923	5.5614				
	4.0	3.9854	5.5933			3.9943 ± 0.0154	99.85
		3.9853	5.5916				
		4.0121	5.6044				
	5.0	4.9615	5.5332			4.9736 ± 0.0207	99.47
		4.9618	5.5839				
		4.9975	5.6097				

output volume and accuracy using the linear model was comparable to that obtained from trained neural network model. The average computation time using the linear model in 5 ml syringe was 7.13 ± 0.02 s for blue-colored syringe tip cap and 5.31 ± 0.05 s for yellow-colored syringe tip cap. Thus on average, using linear model in the 5-ml syringe, the system worked approximately 350 ms faster than that of trained ANN. The efficiency was much higher at the initial, middle, and final data points with the linear model than with the neural network model. As an example with the 5-ml syringe, the recorded efficiency at (158, 0.2), (377, 2.6), and (596, 5.0) points was better with the linear model than with trained neural network model. But for the volume markings in between these points, the trained network provided superior accuracy. This is because of the limited number of data points that are taken into account in the analysis using the linear model. Based on experimental observations, the linear model showed

a small decrease in accuracy but had better computational efficiency. This can impact the use of this system in practical scenarios. Many times injections are drawn through the full scale of volume markings, for example a 3-ml syringe may be used to measure 1, 1.5, 2 ml, etc. Additionally, when measuring highly potent medications, small deviations from the measured volume can significantly affect the dose delivered from a particular volume of injection contained in the syringe. The neural network model considers all the data pairs and trains the network so as to produce the smallest possible error throughout the entire volume range in a syringe.

Computation Time

The computation time includes the time required for the entire process including syringe classification, volume

Table 5 Observed volume, computation time and accuracy for 3 ml syringe with black colored medicine

Syringe size (max. capacity)	Volume in syringe (ml)	Detected volume (ml)	Detection time (s)	Mean \pm SD	Accuracy (%)
Syringe: 3 ml 3 ml	Medicine: black 0.50	0.5686	7.3334	0.5683 \pm 0.0003	86.34
		0.5681	7.4034		
		0.5681	7.5414		
	1.00	0.9998	7.5840	0.9972 \pm 0.0047	99.72
		0.9917	7.3611		
		1.0001	7.8425		
	1.80	1.8108	7.4355	1.8107 \pm 0.0001	99.40
		1.8106	7.6764		
		1.8106	7.6308		
	2.50	2.4379	7.4703	2.4380 \pm 0.0002	97.52
		2.4382	7.3327		
		2.4379	7.3037		
	3.00	3.0155	7.5622	3.0172 \pm 0.0026	99.42
		3.0159	7.3405		
		3.0202	7.4514		
Syringe: 3 ml 3 ml	Medicine: black 0.50	0.5396	5.5282	0.5364 \pm 0.0052	92.72
		0.5392	5.5524		
		0.5305	5.8166		
	1.00	0.9697	5.4774	0.9699 \pm 0.0003	96.99
		0.9699	5.5568		
		0.9702	5.5524		
	1.80	1.7939	5.6081	1.7929 \pm 0.0016	99.60
		1.7910	5.6012		
		1.7938	5.6015		
	2.50	2.4285	5.4699	2.4293 \pm 0.0012	97.17
		2.4286	5.5284		
		2.4307	5.5650		
	3.00	3.0238	5.5351	3.0246 \pm 0.0007	99.18
		3.0250	5.5626		
		3.0250	5.5614		

measurement, and image/output display. The computation time for the core process depends on the microprocessor and system RAM. All experiments were conducted in MATLAB R2013a, which was installed in a computer with Windows 7, 64-bit operating system equipped with Intel Xeon W3550 3.07 GHz processor and 12 GB RAM. During the syringe classification stage when adaptive template matching technique was applied, the computation time for adaptive template matching was dependent on the template size and target image size. For example, computation time for the 5-ml syringe can be seen in Table 4 under the column titled detection time (DT). The mean and standard deviation of these data were calculated, and average detection time for the blue colored syringe tip cap was found to be 7.54 ± 0.04 s, and the average detection time for yellow-colored syringe tip cap was found to be 5.61 ± 0.08 s. The yellow- and blue-colored syringe tip cap

templates possessed similar sizes, so this factor does not seem to significantly contribute to the observed time difference between the two syringe tip caps. The observed time difference is attributed to the manner the algorithm was written. The algorithm sequentially checks for both syringe tip caps, and during the checking step first checks for yellow followed by blue. Thus when checking if the syringe tip cap is yellow, it does not have to check for a blue cap again. But if the syringe tip cap used was blue, first the system checks for the yellow cap followed by the blue cap adding about 2 s to the computation time. This time lag can be reduced by applying parallel processing in the algorithm for adaptive template matching rather than the sequential approach. The time difference noted here was required for single adaptive template matching, but it should be noted that the total computation time additionally includes image acquisition time, image pre-processing

Table 6 Observed volume, computation time and accuracy for 1 ml syringe with red colored medicine

Syringe size (max. capacity)	Volume in syringe (ml)	Detected volume (ml)	Detection time (s)	Mean ± SD	Accuracy (%)		
Syringe: 1 ml		Medicine: red		Syringe tip cap: blue			
1 ml	0.05	0.0492	7.3727	0.0477 ± 0.0012	95.40		
		0.0470	7.3726				
		0.0471	7.3596				
	0.25	0.2414	7.3930			0.2417 ± 0.0003	96.68
		0.2419	7.4112				
		0.2418	7.3493				
	0.50	0.5097	7.3747			0.5097 ± 0.0001	98.06
		0.5097	7.3351				
		0.5097	7.3318				
	0.75	0.7290	7.3771			0.7288 ± 0.0001	97.17
		0.7288	7.3526				
		0.7288	7.4583				
1.00	0.9883	7.3248	0.9894 ± 0.0016	98.94			
	0.9887	7.5294					
	0.9912	7.4016					
Syringe: 1 ml		Medicine: red		Syringe tip cap: yellow			
1 ml	0.05	0.0465	5.5382	0.0453 ± 0.0019	90.60		
		0.0464	5.5694				
		0.0431	5.5918				
	0.25	0.2396	5.6234			0.2397 ± 0.0001	95.88
		0.2399	5.5145				
		0.2397	5.5497				
	0.50	0.5181	5.5226			0.5190 ± 0.0008	96.20
		0.5195	5.5440				
		0.5194	5.7292				
	0.75	0.7253	5.5359			0.7258 ± 0.0009	96.77
		0.7253	5.6733				
		0.7269	5.7401				
1.00	0.9906	5.5530	0.9892 ± 0.0106	98.92			
	0.9990	5.7488					
	0.9780	5.6491					

time, barrel width and plunger depth calculation time. Computation times were recorded for all the trials performed for each syringe. The results suggest that the entire system is computationally efficient and can be realized in real time.

Conclusion

The system for measuring the volume of medication inside Luer-lock syringes comprising SCS and VMS was designed and tested successfully. The syringe classification process helps to differentiate between different sizes of syringes utilized in the compounding process and provides the key input for the volume measurement stage. The best accuracy and precision was observed for the 3-ml syringe (99.95%) with yellow-colored medication and

yellow-colored syringe tip cap. The worst accuracy and precision were found for the 5-ml syringe (95.82%) with colorless medication and blue-colored syringe tip cap. The computational time for the complete process is about 6 s and makes this system realizable in real time. The design of the volume measurement setup uses a web camera, Styrofoam depression for syringe placement, and a high-speed computer. The entire system demonstrated excellent reliability and reproducibility and can be used to monitor the volume of medication present in syringes during aseptic compounding of injections. It can also be utilized to measure the volume of prefilled syringes during quality control testing to verify syringe fill volume. In addition, the algorithm can be customized for automatic volume measurement involving high throughput processes handling liquids in syringes in various industrial settings.

References

- Hatcher I, Sullivan M, Hutchinson J, Thurman S, Gaffney FA. An intravenous medication safety system: preventing high-risk medication errors at the point of care. *J Nurs Adm.* 2004;34(10):437–9.
- Aspden P, Wolcott JA, Bootman JL, Cronenwett LR. Preventing medication errors. National Acad. Press; 2007.
- Yin HS, Mendelsohn AL, Wolf MS, Parker RM, Fierman A, van Schaick L, et al. Parents' medication administration errors: role of dosing instruments and health literacy. *Arch Pediatr Adolesc Med.* 2010;164(2):181–6.
- Kim GR, Chen AR, Arceci RJ, Mitchell SH, Kokoszka KM, Daniel D, et al. Error reduction in pediatric chemotherapy: computerized order entry and failure modes and effects analysis. *Arch Pediatr Adolesc Med.* 2006;160(5):495–8.
- Gudeman J, Jozwiakowski M, Chollet J, Randell M. Potential risks of pharmacy compounding. *Drugs in R&d.* 2013;13(1):1–8.
- Rich D, Fricker M Jr, Cohen M, Levine S. Guidelines for the safe preparation of sterile compounds: results of the ISMP sterile preparation compounding safety summit of October 2011. *Hosp Pharm.* 2013;48(4):282–94. <https://doi.org/10.1310/hpj4804-282>.
- Sasich LD, Sukkari SR. Unknown risks of pharmacy-compounded drugs. *The Journal of the American Osteopathic Association.* 2008;108(2):86–.
- ISMP list of high-alert medications in acute care settings. Institute for Safe Medication Practices 2014. <http://www.ismp.org/tools/highalertmedications.pdf>. Accessed 4 Aug 2017.
- Phillips MS. Standardizing iv infusion concentrations: national survey results. *Am J Health Syst Pharm.* 2011;68(22):2176–82.
- Pedersen CA, Schneider PJ, Scheckelhoff DJ. ASHP national survey of pharmacy practice in hospital settings: dispensing and administration-2011. *Am J Health Syst Pharm.* 2012;69(9):768–85.
- Cantrell SA. Improving the quality of compounded sterile drug products: a historical perspective. *Ther Innov Regul Sci.* 2016;50(3):266–9.
- Wilson M. Sterile compounding pharmacies: states that do and do not require compliance with USP< 797> versus FDA 483s. *Ther Innov Regul Sci.* 2016;50(3):279–303.
- Forcinio H. Trends and best practices in visual inspection: using best practices for manual or automatic inspection can improve the inspection process. *Pharm Technol.* 2014.
- Langille SE. Particulate matter in injectable drug products. *PDA J Pharm Sci Technol.* 2013;67(3):186–200.
- Wichtl M. Herbal drugs and phytopharmaceuticals: a handbook for practice on a scientific basis: CRC press; 2004.
- Chin RT, Harlow CA. Automated visual inspection: a survey. *IEEE Trans Pattern Anal Mach Intell.* 1982;6:557–73.
- Singh S, Bharti M. Image processing based automatic visual inspection system for PCBs. *ISOR J Eng.* 2012;2:1451–5.
- Gunatilake P, Siegel M, Jordan AG, Podnar GW, editors. Image understanding algorithms for remote visual inspection of aircraft surfaces. *Electronic Imaging'97; 1997: International Society for Optics and Photonics.*
- Acquire Images from Webcams. Mathworks, MA, USA. 2016. <http://www.mathworks.com/help/supportpkg/usbwebcams/ug/acquire-images-from-webcams.html>. Accessed 12 Aug 2016.
- Mohr D, Zachmann G, editors. FAST: Fast Adaptive Silhouette Area based Template Matching. *BMVC; 2010.*
- Banharsakun A, Tanathong S. Object detection based on template matching through use of best-so-far ABC. *Comput Intell Neurosci.* 2014;2014:7.
- Wu Z, Goshtasby A. Adaptive image registration via hierarchical voronoi subdivision. *IEEE Trans Image Process.* 2012;21(5):2464–73.
- Roy S, Rathod D. Real-time object tracking and learning using template matching.
- Chantara W, Mun J-H, Shin D-W, Ho Y-S. Object tracking using adaptive template matching. *IEIE Trans Smart Process Comput.* 2015;4(1):1–9.
- Sharmila R, Uma R. A new approach to image contrast enhancement using weighted threshold histogram equalization with improved switching median filter. *Int J Adv Eng Sci Technol.* 2011;7:206–11.
- Otsu N. A threshold selection method from gray-level histograms. *Automatica.* 1975;11(285–296):23–7.
- Cheriet M, Said JN, Suen CY. A recursive thresholding technique for image segmentation. *IEEE Trans Image Process.* 1998;7(6): 918–21.
- Yapa RD, Harada K. A connected component labelling algorithm for greyscale mammography image processing as a pre-processing tool. *Mach Graph Vision Int J.* 2007;16(3):305–27.
- Walczyk R, Armitage A, Binnie D. Comparative study on connected component labeling algorithms for embedded video processing systems. 2010.
- Rudrapatna M, Sowmya A, editors. Feature weighted minimum distance classifier with multi-class confidence estimation. *Australasian Joint Conference on Artificial Intelligence; 2006: Springer.*
- Booth D, Oldfield R. A comparison of classification algorithms in terms of speed and accuracy after the application of a post-classification modal filter. *Remote Sens.* 1989;10(7):1271–6.
- Gerstner W. Supervised learning for neural networks: a tutorial with Java Exercises. Recurso disponible on-line: <http://diwww.epfl.ch/mantra/tutorial/english/supervised.pdf>. 1998.
- Fine S, Scheinberg K. Efficient SVM training using low-rank kernel representations. *J Mach Learn Res.* 2001;2(Dec):243–64.
- Vlacic L. Learning and soft computing, support vector machines, neural networks, and fuzzy logic models. Vojislav Kecman; MIT Press, Cambridge, MA, 2001, ISBN 0-262-11255-8, 2001, pp. 578. Elsevier; 2002.
- Yu H, Wilamowski BM. Levenberg-Marquardt training. *Ind Electron Handb.* 2011;5(12):1.